Self-referential holography and its applications to data storage and phase-to-intensity conversion

Masanori Takabayashi[1,*] and Atsushi Okamoto[2]

[1]*Department of Systems Design and Informatics, Kyushu Institute of Technology, 680-4 Kawazu, Iizuka, Fukuoka 820-8502, Japan*

[2]*Graduate School of Information Science and Technology, Hokkaido University, North 14 West 9, Kita-ku, Sapporo 060-0814, Japan*

[*]*takabayashi@ces.kyutech.ac.jp*

Abstract: Holographic recording methods require the use of a reference beam that is coherent with the signal beam carrying the information to be recorded. In this paper, we propose self-referential holography (SRH) for holographic recording without the use of a reference beam. SRH can realize purely one-beam holographic recording by considering the signal beam itself as the reference beam. The readout process in SRH is based on energy transfer by inter-pixel interference in holographic diffraction, which depends on the spatial phase difference between the recorded phase and the readout phase. The phase-modulated recorded signal is converted into an intensity-modulated beam that can be easily detected using a conventional image sensor. SRH can be used effectively for holographic data storage and phase-to-intensity conversion.

OCIS codes: (090.0090) Holography; (210.2860) Holographic and volume memories.

References and links

1. D. Gabor, "A new microscopic principle," Nature **161**(4098), 777–778 (1948).
2. N. Peyghambarian, S. Tay, P.-A. Blanche, R. Norwood, and M. Yamamoto, "Rewritable holographic 3D displays," Opt. Photon. News **19**(7), 22–27 (2008).
3. P. A. Blanche, A. Bablumian, R. Voorakaranam, C. Christenson, W. Lin, T. Gu, D. Flores, P. Wang, W. Y. Hsieh, M. Kathaperumal, B. Rachwal, O. Siddiqui, J. Thomas, R. A. Norwood, M. Yamamoto, and N. Peyghambarian, "Holographic three-dimensional telepresence using large-area photorefractive polymer," Nature **468**(7320), 80–83 (2010).
4. P. J. van Heerden, "Theory of optical information storage in solids," Appl. Opt. **2**(4), 393–400 (1963).
5. D. Psaltis and G. W. Burr, "Holographic data storage," Computer **31**(2), 52–60 (1998).
6. H. Horimai, X. Tan, and J. Li, "Collinear holography," Appl. Opt. **44**(13), 2575–2579 (2005).
7. K. Curtis, L. Dhar, A. J. Hill, W. L. Wilson, and M. R. Ayres, *Holographic Data Storage: From Theory to Practical Systems* (John Wiley & Sons, 2010).
8. D. Malacara, *Optical Shop Testing – Third Edition* (Wiley-Interscience, 2007).
9. I. Yamaguchi and T. Zhang, "Phase-shifting digital holography," Opt. Lett. **22**(16), 1268–1270 (1997).
10. Y. Awatsuji, M. Sasada, and T. Kubota, "Parallel quasi-phase-shifting digital holography," Appl. Phys. Lett. **85**(6), 1069–1071 (2004).
11. J. Joseph and D. A. Waldman, "Homogenized Fourier transform holographic data storage using phase spatial light modulators and methods for recovery of data from the phase image," Appl. Opt. **45**(25), 6374–6380 (2006).
12. P. Koppa, "Phase-to-amplitude data page conversion for holographic storage and optical encryption," Appl. Opt. **46**(17), 3561–3571 (2007).
13. H. Kato, H. Horimai, P. B. Lim, K. Watanabe, M. Inoue, R. Arai, N. Morishita, and J. Ikeda, "Multi-level phase recording by collinear phase-lock holography," Proceedings of International Workshop on Holographic Memories & Display, 79–80 (2009).
14. E. N. Leith and J. Upatnieks, "Reconstructed wavefronts and communication theory," J. Opt. Soc. Am. **52**(10), 1123–1128 (1962).
15. Y. N. Denisyuk, "Photographic reconstruction of the optical properties of an object in its own scattered radiation field," Sov. Phys. Dokl. **7**, 543–545 (1962).
16. H. Kogelnik, "Coupled-wave theory for thick hologram grating," Bell Syst. Tech. J. **48**, 2909–2947 (1969).
17. M. D. Feit and J. A. Fleck, Jr., "Light propagation in graded-index optical fibers," Appl. Opt. **17**(24), 3990–3998 (1978).

#179394 - $15.00 USD Received 6 Nov 2012; revised 19 Jan 2013; accepted 29 Jan 2013; published 6 Feb 2013

18. S. Ahmed and E. N. Glytsis, "Comparison of beam propagation method and rigorous coupled-wave analysis for single and multiplexed volume gratings," Appl. Opt. **35**(22), 4426–4435 (1996).
19. J. Tanaka, A. Okamoto, and M. Kitano, "Development of image-based simulation for holographic data storage system by fast Fourier transform beam-propagation method," Jpn. J. Appl. Phys. **48**(3), 03A028 (2009).
20. C. Katahira, N. Morishita, J. Ikeda, P. B. Lim, M. Inoue, Y. Iwasaki, H. Aota, and A. Matsumoto, "Mechanistic discussion of cationic crosslinking copolymerizations of 1,2-epoxycyclohexane with diepoxide crosslinkers accompanied by intramolecular and intermolecular chain transfer reactions," J. Polym. Sci. A Polym. Chem. **48**, 4445–4455 (2010).

1. Introduction

Since its invention by Gabor in 1948 [1], holography has been widely researched and has led to the development of various technologies, for instance, display [2, 3], data storage [4–7], and measurement [8–10]. One common feature of these technologies is that in order to record an optically generated hologram, a reference beam that is coherent with the signal beam carrying the information to be recorded is required. However, the need for a coherent reference beam complicates the recording optics and introduces limitations.

To avoid increasing the number of optical elements and overall complexity, we propose a novel hologram recording method, self-referential holography (SRH). SRH provides two attractive features: 1) purely one-beam hologram recording without a reference beam and 2) direct data detection of recorded phase-modulated signals without using phase detection methods, which are necessary for several applications such as phase-modulated holographic data storage [11–13]. The first feature, purely one-beam hologram recording, is achieved by regarding the signal beam, which is spatially phase modulated, as the reference beam, allowing the signal beam to record itself. In conventional holography, if the signal beam were to serve as both the information-carrying beam and the reference beam for recording, the hologram cannot be reconstructed without the information on the signal beam used for recording. In contrast, SRH enables read out of the recorded signal data by the appropriate phase-modulated wave irradiation. The second feature of SRH corresponds to the fact that the recorded phase-modulated signals are read out as an intensity-modulated beam with the same spatial pattern as the phase difference pattern between the writing beam and the readout beam. The reason is that the SRH readout process is based on energy transfer between pixels in the diffracted readout beam, which depends on the inter-pixel phase difference between the phase distributions of the recording and readout beams. The observed intensity of a specific data pixel depends on whether constructive or destructive coupling arises between the transmission component of the pixel and the diffraction component of its surrounding pixels, which propagate in the same direction. This is the biggest difference between SRH and conventional holography schemes such as the in-line [1], Leith [14], Denisyuk [15], and coaxial holography [6] schemes.

Typical applications enabled by these attractive advantages of SRH include holographic data storage. SRH-based holographic data storage can be realized in almost the same way as in conventional optical storage system technologies such as Blu-ray. Furthermore, in SRH-based holographic data storage, the entire beam area that is incident on the objective lens can be used only for signals, whereas only part of the beam is used in coaxial holography, owing to the allocation of the reference beam [6]. Therefore, the data transfer rate in SRH-based holographic data storage is expected to be higher than that in coaxial holographic data storage. In addition, no phase detection method is required for SRH because the recorded phase-modulated signals are read out as intensity-modulated signals. This feature has a possibility to solve the problem in phase-based holographic data storage in which phase detection or phase-to-intensity conversion (PIC) methods cause complexities of optics [11–13]. The applications of SRH are not limited to optical data storage alone: We can also expect applications to holographic diffraction elements and optical security systems. Among the potential applications, high-speed PIC is one of the most effective uses of SRH.

#179394 - $15.00 USD Received 6 Nov 2012; revised 19 Jan 2013; accepted 29 Jan 2013; published 6 Feb 2013

In this paper, we describe the principle of SRH theoretically and prove the principle by numerical simulation and experiment. The theory, which is based on Kogelnik's coupled-wave theory [16], provides a clear understanding of SRH by assuming the simplest model. However, this model is not rigorous because it completely neglects practical conditions such as the effects of the lens aperture and inter-pixel crosstalk noise. To prove that SRH operates even under more practical conditions, we perform numerical simulations based on the fast Fourier transform beam-propagation method (FFT-BPM) [17–19] and experiments using photopolymer materials. In the experiments, a signal-to-noise ratio (SNR) of more than 3.0 dB can be obtained in storage-type SRH.

2. Self-referential holography

In SRH, holograms are recorded and read out in a different way than in conventional holography. Recording and readout of holograms in SRH are achieved with only one beam, the area of which need not be divided into multiple areas. This is possible because of the characteristic methods of recording and reading out holograms. An example of the optical geometry of SRH is shown in Figs 1(a) and 1(b). In the recording process, holograms are generated by self-interference of a phase-modulated writing beam. In other words, a pixel of the writing beam interferes with the other pixels, for example, when the writing beam is focused by an objective lens. In contrast, the SRH readout process is based on energy interchanges between pixels in the readout beam, which occur when the appropriate phase difference pattern exists between the writing and readout beams. We give an overview of the fundamental procedures of SRH in subsection 2.1 and explain the principle of SRH theoretically in subsection 2.2. We suggest holographic data storage (storage-type SRH) and PIC (PIC-type SRH) as examples of applications of SRH.

2.1 Fundamental procedures in self-referential holography

The most important thing in SRH is controlling the phase distributions that are added to a laser beam. Here, we explain the fundamental procedures for recording and detecting the signal pattern $\phi^s(x, y)$ in storage-type operation and PIC-type operation, respectively. In this paper, we assume optics in which a spatial light modulator (SLM), an objective lens, and a recording medium are separated by a distance corresponding to the focal length of the objective lens: i.e., the SLM, objective lens in front of the recording medium, recording medium itself, objective lens behind the recording medium, and imager are arranged in a 4-*f* optical geometry.

In the recording process in storage-type SRH, first, the writing pattern $\phi^w(x, y)$ is computationally generated from a binary pattern $\phi^s(x, y)$ and an additional pattern $\phi^{ad}(x, y)$. The binary pattern $\phi^s(x, y)$ represents the signal to be recorded and read out, and the additional pattern $\phi^{ad}(x, y)$ is used to read out the signal pattern $\phi^s(x, y)$ during readout. Here, the additional pattern $\phi^{ad}(x, y)$ does not need to be binary; any number of levels including a uniform pattern is acceptable. The writing pattern $\phi^w(x, y)$ is displayed on the phase-only SLM during recording and is added to the laser beam as a phase-modulated pattern. Thus, the complex amplitude of the writing beam behind the SLM becomes

$$\begin{aligned} E^w_{SLM}(x,y) &= A^w \exp\left[i\phi^w(x,y) \right] \\ &= A^w \exp\left\{ i\left[\phi^s(x,y) + \phi^{ad}(x,y) \right] \right\}. \end{aligned} \tag{1}$$

A^w is the amplitude of the writing beam, which is spatially uniform. After passing through the SLM, the writing beam $E^w_{SLM}(x, y)$ is focused by an objective lens and interferes with the writing beam itself, as shown in Fig. 1(a). Therefore, holograms can be generated without any reference beam when the recording medium is set near the focal plane of the objective lens. This is one of the notable features of SRH: hologram recording by self-interference.

#179394 - $15.00 USD Received 6 Nov 2012; revised 19 Jan 2013; accepted 29 Jan 2013; published 6 Feb 2013

During readout of storage-type SRH, the readout pattern $\phi^r(x, y)$ is displayed on the phase-only SLM. Then, to read out the signal pattern $\phi^s(x, y)$, the readout pattern $\phi^r(x, y)$ has to be the same as the additional pattern $\phi^{ad}(x, y)$ used in the recording process. If the readout pattern does not correspond to the additional pattern, the readout pattern would be uniform. Therefore, the complex amplitude of the readout beam behind the SLM can be written as

$$\begin{aligned} E^r_{SLM}(x,y) &= A^r \exp\left[i\phi^r(x,y)\right] \\ &\equiv A^r \exp\left[i\phi^{ad}(x,y)\right]. \end{aligned} \tag{2}$$

As in the recording process, A^r is the amplitude of the readout beam and is spatially uniform. As shown in Fig. 1(b), the readout beam $E^r_{SLM}(x, y)$ illuminates the holograms in the same manner as in the recording process. When the readout beam is illuminated, energy is interchanged between the pixels in the readout beam. The details of the energy interchanges are described in subsection 2.2 and depend on the relative phase difference between the writing and readout beams. Because the readout pattern $\phi^r(x, y)$ is the same as the additional phase pattern $\phi^{ad}(x, y)$, the phase difference pattern between the writing and readout beams, $\phi^r(x, y) - \phi^w(x, y)$, corresponds to the signal pattern $-\phi^s(x, y)$. The energy interchanges, which thus depend on the signal pattern $-\phi^s(x, y)$ produce the binary intensity pattern $I^s(x, y)$ on the imager plane with the same distribution as the binary signal pattern $-\phi^s(x, y)$. As a result, SRH can be used as optical storage with attractive features, in which the signal pattern $\phi^s(x, y)$ is recorded as phase-modulated signals and read out as intensity-modulated signals.

In addition to storage-type operation, SRH can be applied in a phase-to-intensity convertor, which can instantly convert a binary phase-modulated beam to an intensity-modulated beam. The optical arrangement of PIC-type SRH is similar to that of phase contrast microscopy. However, their principles differ from each other. PIC-type SRH converts the phase-modulated image to an intensity-modulated image by inter-pixel interaction of the image, whereas phase contrast microscopy performs conversion by interference between two different images. In PIC-type SRH, the writing phase pattern $\phi^w(x, y)$ and the readout phase pattern $\phi^r(x, y)$ are inversely displayed on the phase-only SLM, as shown in Fig. 1(c). In the recording process, the holograms are generated by illumination with a beam having the complex amplitude

$$E^w_{SLM}(x,y) = A^w \exp\left[i\phi^r(x,y)\right]. \tag{3}$$

As in storage-type SRH, the amplitude A^w should be spatially uniform. The generated holographic optical element works as a phase-to-intensity convertor for the phase-modulated beam,

$$\begin{aligned} E^r_{SLM}(x,y) &= A^r \exp\left[i\phi^w(x,y)\right] \\ &= A^r \exp\left\{i\left[\phi^s(x,y) + \phi^{ad}(x,y)\right]\right\}. \end{aligned} \tag{4}$$

As described above, in SRH, the energy interchanges, which depend on the relative phase difference between the writing and readout beams, permit the conversion of the signal phase pattern to a signal intensity patterns. In PIC-type SRH, the difference in phase patterns between the writing and readout beams, $[\phi^s(x, y) + \phi^{ad}(x, y)] - \phi^r(x, y)$, becomes $\phi^s(x, y)$ when $\phi^r(x, y) = \phi^{ad}(x, y)$ is satisfied. Note that the phase difference in storage-type SRH, $-\phi^s(x, y)$, and that in PIC-type SRH, $\phi^s(x, y)$, have opposite signs. Thus, the obtained intensity patterns $I^s(x, y)$ are also reversed, as shown in Fig. 1(c). As a result, SRH can also be used as a phase-to-intensity converter that provides high-speed conversion from a binary phase pattern to an intensity pattern.

#179394 - $15.00 USD Received 6 Nov 2012; revised 19 Jan 2013; accepted 29 Jan 2013; published 6 Feb 2013

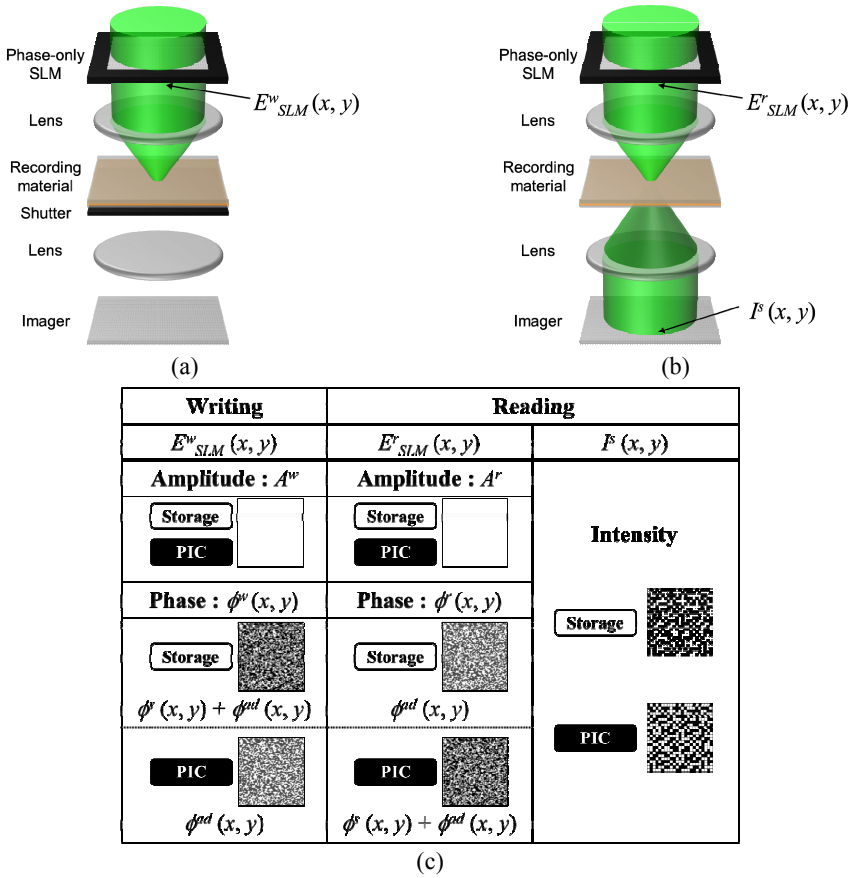

Fig. 1. Conceptual diagram of self-referential holography. (a) Optical geometry for recording. The writing beam with a complex amplitude of $E^w_{SLM}(x, y)$ is focused by an objective lens, and holograms are generated by self-interference between recording pixels. (b) The readout beam with a complex amplitude of $E^r_{SLM}(x, y)$ is focused by an objective lens. The uniform readout intensity is changed to the signal intensity pattern $I^s(x, y)$ via the energy interchanges in the holograms. (c) Complex amplitudes of writing and readout beams. The patterns $\phi^w(x, y)$ and $\phi^r(x, y)$ are added to the writing and readout beams, respectively. If $\phi^w(x, y) - \phi^r(x, y) \equiv \pm \phi^s(x, y)$, the intensity pattern that corresponds to the distribution of $\pm \phi^s(x, y)$ can be observed.

2.2 Coupled wave equations for self-referential holography

To clarify the principle of the energy interchanges occurring during SRH readout, we derive the coupled wave equations. In what follows, we assume that the light from the pixels of the SLM is transformed to plane waves by the objective lens. These plane waves interfere with each other and generate holograms, as shown in Fig. 2(a). In addition, we regard the SLM pattern, e.g., $\phi^w(x, y)$, as a set of spatially discretized points, ϕ_p^w $(1 \le p \le N)$, as shown in Fig. 2(b). Here N is the number of pixels in the SLM. Thus, to represent the p-th pixel of the writing pattern, we use the expression ϕ_p^w instead of $\phi^w(x, y)$. This rule is applied to the other distributions such as $\phi^s(x, y)$, $\phi^{ad}(x, y)$, and $\phi^r(x, y)$.

During recording, the pixels of the writing beam are converted to plane waves by the objective lens, which accepts them when the 4-*f* geometry is used. These plane waves reach the surface of the recording medium; the resulting complex amplitude can be written as

$$E^w(\mathbf{r}, t) = \sum_{p=1}^{N} A_p^w \exp\left[i\left(\omega t - \mathbf{k}_p \cdot \mathbf{r} + \psi_p^w \right) \right]. \tag{5}$$

#179394 - $15.00 USD Received 6 Nov 2012; revised 19 Jan 2013; accepted 29 Jan 2013; published 6 Feb 2013

The number of plane waves equals that of SLM pixels, N. A_p^w, $\boldsymbol{k}_p$, and ψ_p^w are the amplitude, wave vector, and phase on the surface of the recording medium of the beam from the p-th SLM pixel, respectively. Further, i is the imaginary unit, ω is the angular frequency, t is the time, and $\boldsymbol{r}$ is the positional vector. The plane waves described by Eq. (5) generate the holograms, which can be written as

$$n(r) = n_0 + \sum_{1 \le m < n < N} n_{mn} \cos\left[\mathbf{K}_{mn} \cdot \mathbf{r} - \Delta\psi_{mn}^w \right] \tag{6}$$

Here n_0 and n_{mn} are the steady component and perturbation component of the hologram, respectively, which is generated by the m-th and n-th plane waves. $\boldsymbol{K}_{mn}$ and $\Delta\psi_{mn}^w$ are the grating wave vector and initial phase difference between the m-th and n-th plane waves, respectively, and can be described by

$$\mathbf{K}_{mn} = \mathbf{k}_n - \mathbf{k}_m, \tag{7}$$

$$\Delta\psi_{mn}^w = \psi_n^w - \psi_m^w. \tag{8}$$

In Eq. (7), the $2K$, $3K$ ... diffraction gratings are neglected.

During readout, the readout pattern is converted to many plane wave components,

$$E^r(\mathbf{r}, t) = \sum_{p=1}^{N} A_p^r \exp\left[i\left(\omega t - \mathbf{k}_p \cdot \mathbf{r} + \psi_p^r \right) \right]. \tag{9}$$

By substituting Eq. (6) and Eq. (9) in the following wave equation

$$\left\{ \nabla^2 + \left[\frac{2\pi}{\lambda} n(r) \right] - i\omega\mu\sigma \right\} E^r(\mathbf{r}, t) = 0, \tag{10}$$

the coupled wave equations for SRH can be obtained as follows:

$$\begin{aligned}
&\left(\frac{d}{dz} + \frac{\alpha}{\cos\theta_1} \right) A_1^r = \frac{-i}{\cos\theta_1} \left[\sum_{q=2}^{N} \kappa_{1q} A_q^r \exp\left(-i\Delta\psi_{1q} \right) \right] \\
&\qquad \vdots \\
&\left(\frac{d}{dz} + \frac{\alpha}{\cos\theta_{p0}} \right) A_{p0}^r = \frac{-i}{\cos\theta_{p0}} \left[\sum_{q=1}^{p0-1} \kappa_{qp0} A_q^r \exp\left(i\Delta\psi_{qp0} \right) + \sum_{q=p0+1}^{N} \kappa_{p0q} A_q^r \exp\left(-i\Delta\psi_{p0q} \right) \right] \\
&\qquad \vdots \\
&\left(\frac{d}{dz} + \frac{\alpha}{\cos\theta_N} \right) A_N^r = \frac{-i}{\cos\theta_N} \left[\sum_{q=1}^{N-1} \kappa_{qN} A_q^r \exp\left(i\Delta\psi_{qN} \right) \right].
\end{aligned} \tag{11}$$

Here z is the thickness direction of the recording medium, and α and κ_{mn} are an absorption coefficient and a coupling coefficient, respectively. They can be written as

$$\alpha = \frac{\mu c \sigma}{2 n_0}, \tag{12}$$

$$\kappa_{mn} = \frac{\pi n_{mn}}{\lambda}. \tag{13}$$

In addition, θ_{p0} is the angle between the p_0-th readout beam and the z axis, which is normal to the medium surface. Note that $\Delta\psi_{mn}$ is defined as the phase difference on the surface of the recording medium; however, this corresponds to that on the SLM plane,

#179394 - $15.00 USD Received 6 Nov 2012; revised 19 Jan 2013; accepted 29 Jan 2013; published 6 Feb 2013

$$\begin{aligned}\Delta\psi_{mn} &= \Delta\psi^{r}_{mn} - \Delta\psi^{w}_{mn} \\ &= \Delta\phi^{r}_{mn} - \Delta\phi^{w}_{mn} \\ &= \Delta\phi_{mn}.\end{aligned} \tag{14}$$

From Eq. (11), the derivation of the p_0-th plane wave along the z axis, the thickness direction of the recording medium $dA^{r}_{p_0}/dz$ can be described by the superposition of contributions from the other waves. If all the coupling coefficients have the same sign, the sign of $dA^{r}_{p_0}/dz$ depends only on the phase difference $\Delta\phi_{mn}$.

To solve the coupled wave equations in Eq. (11), we assume the conditions shown in Fig. 3(a). We used a binary pattern with a phase difference of π/2 as the signal pattern $\phi^{s}(x, y)$. Both the additional pattern $\phi^{ad}(x, y)$ and the readout pattern $\phi^{r}(x, y)$ were set to be uniform. Here we calculate the changes in the intensity of each plane wave for storage-type SRH. The intensity changes along the z axis are shown in Fig. 3(b). The intensities of all the pixels were divided into two levels: higher and lower than those of the input readout beam. Furthermore, the obtained intensities at the output depend on the signal phase levels.

For a conceptual understanding of the principle of SRH, we consider the simplest case: the number of SLM pixels $N = 2$, the writing phase of pixel 1 $\phi_1^{w} = 0$ or π/2, that of pixel 2 $\phi_2^{w} = 0$ or π/2, the reading phase of pixel 1 $\phi_1^{r} = 0$, that of pixel 2 $\phi_2^{r} = 0$. After the hologram is recorded, the readout beams illuminate it. According to diffraction theory, diffraction involves phase shifting by π/2. In addition to the phase shifting due to diffraction, because the two readout beams see that the hologram has a spatial phase shift of $\phi = \phi_1^{w} - \phi_2^{w}$, the diffracted beam on one side involves a phase shift of $-\phi$, whereas that on the other side involves a phase shift of ϕ. Consequently, the zeroth-order diffraction component of one beam is coupled with the first-order diffraction component of the other beam with a phase difference of $\pi/2 + \phi$ on one side, whereas the first-order component of one beam is coupled with the first-order component of the other beam with a phase difference of $\pi/2 - \phi$ on the other side. Therefore, the output intensities of these two pixels, I_1 and I_2, are divided into three cases: $I_1 < I_2$ ($\phi_1^{w} = 0$, $\phi_2^{w} = \pi/2$), $I_1 = I_2$ ($\phi_1^{w} = \phi_2^{w}$), and $I_1 > I_2$ ($\phi_1^{w} = \pi/2$, $\phi_2^{w} = 0$). This shows that the recorded phase difference is converted to an intensity difference.

In addition to the simplest case, we consider a more practical case in which the SLM has more than three pixels: the number of SLM pixels $N = 4$, the writing phase of pixel 1 $\phi_1^{w} = 0$, that of pixel 2 $\phi_2^{w} = \pi/2$, that of pixel 3 $\phi_3^{w} = 0$, that of pixel 4 $\phi_4^{w} = \pi/2$, and the phases of all the reading pixels ϕ_1^{r}, ϕ_2^{r}, ϕ_3^{r}, $\phi_4^{r} = 0$. Figure 4 shows conceptually the amplitude change of each readout pixel. Before propagating inside the holograms, these four pixels have the same amplitude. During propagation inside the six holograms, H_{12}, H_{13}, H_{14}, H_{23}, H_{24}, and H_{34}, the amplitudes are changed by coupling with the other beams. Here, H_{XY} denotes the hologram that is generated by the beams from pixels X and Y in the recording process. The arrow in Fig. 4 shows the direction of energy transfer, which depends on the relationship between the phase distributions of the writing beam and the readout beam. In addition, the amount of energy transfer is determined by the diffraction efficiency of the hologram. Here we should note that even when the diffraction efficiency of each hologram is low, the contrast of the output image would remain high if there were many SLM pixels. This means that the refractive index modulation depth, which affects the diffraction efficiency, needs not to be large if there are many SLM pixels. If the required refractive index modulation depth is small, the number of recordable holograms by multiplexing will increase.

However, the results described above are not rigorous because effects such as those of the lens aperture, diffraction at the SLM pixels, and inter-pixel crosstalk were completely neglected in the derivation of the coupled wave equations. Even under the more practical case when a beam is diffracted by the hologram generated by the beam itself, we should confirm

#179394 - $15.00 USD Received 6 Nov 2012; revised 19 Jan 2013; accepted 29 Jan 2013; published 6 Feb 2013

the SRH operations. By performing simulations based on FFT-BPM and experiments, we show the SRH operation in more practical situations.

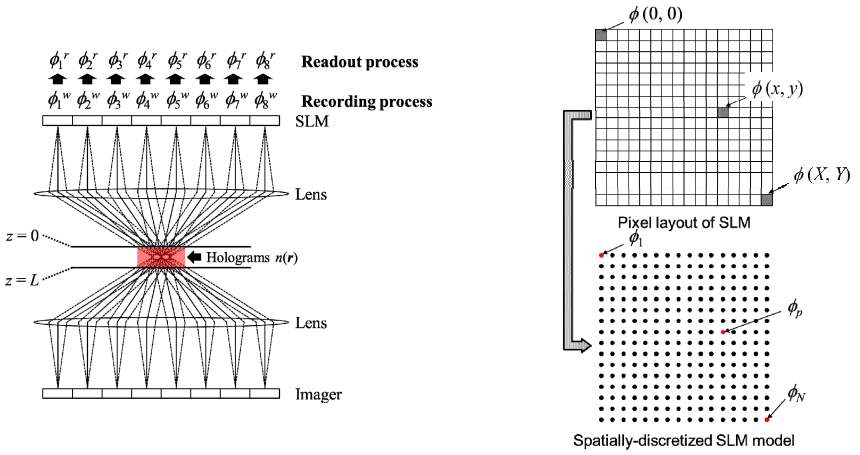

Fig. 2. Models for theoretical description of SRH principle. (a) Overview of the model. Light from the SLM pixels is converted to plane waves by a lens. These plane waves interfere with each other, and holograms are generated. (b) Layout of SLM. In the theoretical description, the pixels of the SLM are regarded as a set of many point sources.

The number of pixels	N	50
Signal pattern	$\phi^s(x, y)$	0 or $\pi/2$
Additional pattern	$\phi^{ad}(x, y)$	0
Writing pattern	$\phi^w(x, y)$	0 or $\pi/2$
Readout pattern	$\phi^r(x, y)$	0

(a)

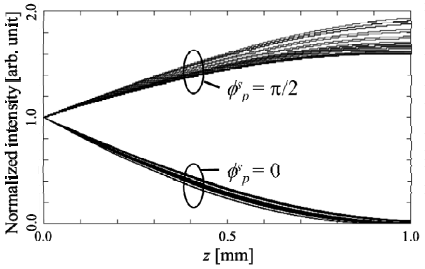

(b)

Fig. 3. (a) Conditions for solving the coupled wave equations. (b) Output intensity changes obtained from the coupled wave equations. The intensities of all pixels having the same intensity before illuminating the holograms ($z = 0.0$) are different at the output ($z = 1.0$).

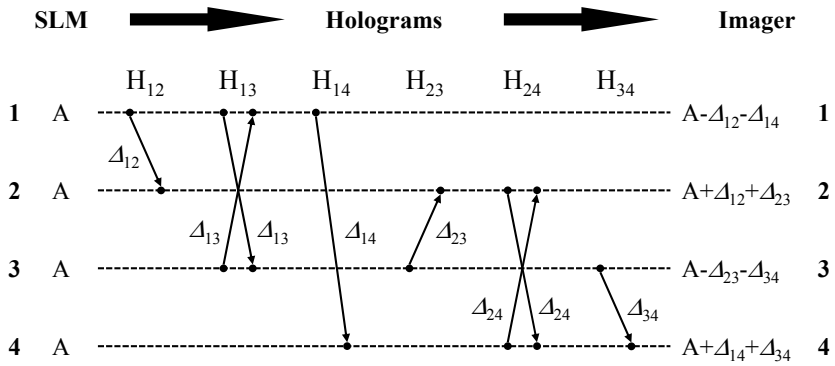

Fig. 4. Conceptual diagram of energy interchanges between four pixels. In this example, the intensities of pixels 1 and 3 are lower than those of pixels 2 and 4 at the output.

#179394 - $15.00 USD Received 6 Nov 2012; revised 19 Jan 2013; accepted 29 Jan 2013; published 6 Feb 2013

3. Numerical simulations and experiments

In the previous section, we described the fundamental SRH operations. In particular, the results shown in Fig. 3, which were obtained by deriving the coupled wave equations, provided a good understanding of these operations. However, the coupled wave equations are introduced by assuming that only the beam is diffracted by the hologram that generates the beam. Thus, this theory did not consider a practical case, for example, the effects of the lens aperture, diffraction at the SLM pixels, and inter-pixel crosstalk noise. Therefore, in this section, numerical simulations and experiments are performed to investigate more practical SRH operation.

3.1 Numerical simulations

We performed numerical simulations to investigate more practical SRH operation. We confirmed storage-type operation, in which the signal pattern $\phi^s(x, y)$ can be recorded as a phase-modulated signal and read out as an intensity-modulated signal, and PIC-type operation, in which the phase pattern $\phi^s(x, y)$ can be quickly converted to an intensity-modulated signal only by passing through the holograms. The models of the simulations are illustrated in Fig. 5. Light propagation inside the holograms was calculated by using the FFT-BPM. In addition, we did not treat hologram multiplexing. The parameters are as follows: the recording beam power was 0.1 mW, the wavelength was 408.0 nm, the SLM had 50 × 50 pixels with a pixel pitch of 30 μm, the focal length of the objective lens was 1.1 mm, the thickness of the recording material was 400 μm, and the maximum refractive index modulation depth was 4.0×10^{-3}.

During recording in storage-type SRH, the signal pattern $\phi^s(x, y)$ and the additional pattern $\phi^{ad}(x, y)$ are computationally summed and displayed on the phase-only SLM. The displayed pattern, $\phi^w(x, y) = \phi^s(x, y) + \phi^{ad}(x, y)$, is shown in Fig. 6(c), where the signal pattern $\phi^s(x, y)$ and the additional pattern $\phi^{ad}(x, y)$ are shown in Figs. 6(a) and 6(b), respectively. Here we assume that the phase-only SLM provides a phase delay to the input beam linearly. The signal pattern $\phi^s(x, y)$ has 2 phase levels with a difference of $\pi/2$, whereas the additional pattern has 2 phase levels. When the writing beam $E^w(x, y) = \exp[i\pi\phi^w(x, y)]$ is focused by an objective lens, the interference pattern $I(x, y, z)$ is distributed inside the recording medium. The interference pattern can be converted to the refractive index grating $\Delta n(x, y, z)$ as follows:

$$\Delta n(x, y, z) = \Delta n_{\max} \left\{ 1 - \exp\left[-\frac{I(x, y, z) \cdot T}{G_{sat}} \right] \right\}. \tag{15}$$

Here, $\Delta n_{\max}$ is the maximum refractive index modulation depth of the material, T is the recording time, and G_{sat} is the energy saturation flux density.

During readout in storage-type SRH, the readout pattern $\phi^r(x, y)$, which is shown in Fig. 6(b), is displayed on the phase-only SLM. Note that $\phi^r(x, y) = \phi^{ad}(x, y)$ is satisfied. The readout beam $E^r(x, y) = \exp[i\pi\phi^r(x, y)]$ propagates inside the holograms, which are generated in the recording process. The propagation of the readout beam was calculated using the FFT-BPM. By inversely Fourier transforming the complex amplitude after propagation, the intensity distribution on the imager plane can be obtained, as shown in Fig. 6(d). The pixels with stronger and weaker intensity correspond to those with phase levels of $\pi/2$ and 0, respectively. The quality of the output intensity patterns is evaluated using the SNR, which is defined as

$$SNR = \frac{I_{ON} - I_{OFF}}{\sqrt{\sigma_{ON}^2 + \sigma_{OFF}^2}}. \tag{16}$$

#179394 - $15.00 USD Received 6 Nov 2012; revised 19 Jan 2013; accepted 29 Jan 2013; published 6 Feb 2013

Here, the pixels having a phase value of π/2 during recording are called ON pixels, and those having the phase value of 0 are OFF pixels. I_{ON} and I_{OFF} denote the average output intensities of ON and OFF pixels, respectively, and σ_{ON} and σ_{OFF} denote the standard deviations of ON and OFF pixels, respectively. The SNR of the output intensity pattern shown in Fig. 6(d) was 4.09.

The operation of PIC-type SRH can be simulated in the same manner. In PIC-type SRH, the pattern shown in Fig. 6(c) is displayed on the SLM during recording, whereas that shown in Fig. 6(b) is displayed during readout. Then the phase pattern shown in Fig. 6(a) is instantly converted to the corresponding intensity patterns, as shown in Fig. 6(e). The pixels with stronger and weaker intensity correspond to those with phase levels of 0 and π/2, respectively. The SNR of the converted pattern was −2.90. Note that the SNR of PIC-type SRH has a negative value. This is because the sign of the phase difference patterns between the writing and readout beams in storage-type SRH and PIC-type SRH are opposite, as described in section 2.

In this simulation, we could confirm SRH operation with a relatively high SNR. One of the ways to achieve a higher SNR in a single-page SRH, the reduction of inter-pixel crosstalk noise, is particularly important. Inter-pixel crosstalk in SRH occurs when the unrequired holograms diffract light. In other words, holograms in SRH can be regarded as multiplexing of many plane wave holograms. Therefore, all the holograms generated by plane waves should be isolated by Bragg's condition. However, the angles of these plane waves depend on the position of the SLM pixels; therefore, the holograms cannot be considered independently. Obviously, increasing the inter-pixel distances of the SLM pixels is an effective solution, but this limits, for example, the data access rate in storage-type SRH. Thus, we can reduce the influence of the inter-pixel crosstalk noise, although it cannot be eliminated. To improve the SNR, the angular selectivity of each plane wave hologram should be made tighter, for example, by using a thicker recording medium.

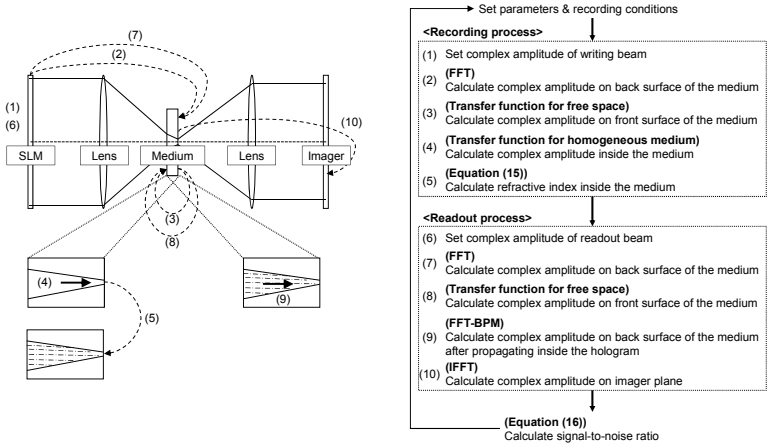

Fig. 5. Models and flows in FFT-BPM-based simulations.

#179394 - $15.00 USD Received 6 Nov 2012; revised 19 Jan 2013; accepted 29 Jan 2013; published 6 Feb 2013

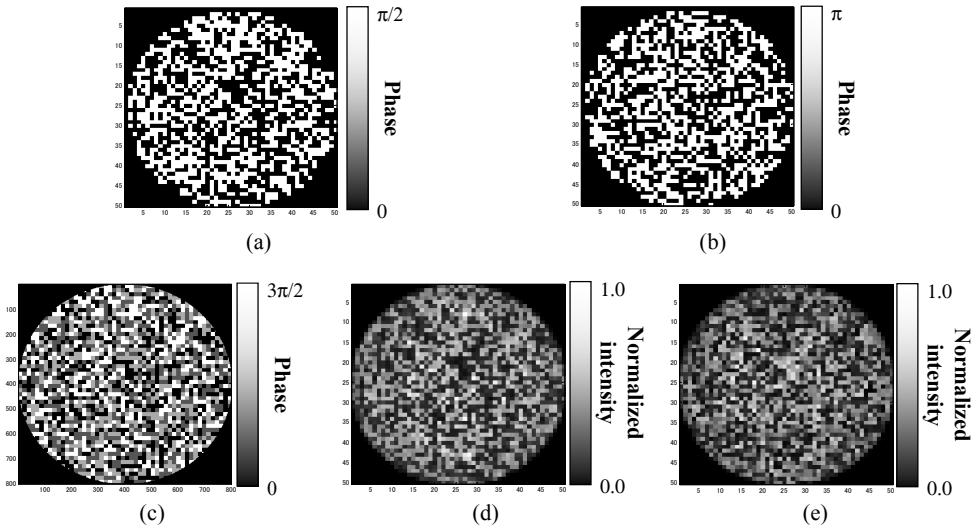

Fig. 6. Simulation results. (a) Signal pattern $\phi^{s}(x, y)$. This pattern is used as the signal to be recorded in storage-type SRH and as the target to be detected in PIC-type SRH. (b) Additional pattern $\phi^{ad}(x, y)$. This pattern is recorded in PIC-type SRH. (c) Writing pattern $\phi^{w}(x, y) = \phi^{s}(x, y) + \phi^{ad}(x, y)$ for storage-type SRH. Readout pattern for PIC-type SRH. (d) Normalized output intensity pattern of storage-type SRH. (e) Normalized output intensity pattern of PIC-type SRH.

3.2 Experiments

Experiments on both storage-type and PIC-type SRH were conducted. In the experimental setup, which is shown in Fig. 7, the beam from a diode-pumped solid-state laser with a wavelength of 532.0 nm is expanded, and the writing pattern is phase-modulated to the laser beam by a reflection-type SLM (LC-R 1080, Holoeye). The signal is focused by an objective lens with a numerical aperture of 0.65 and focal length of 4.5 mm. The recording intensity was 115 μW/cm^2. Here we used a photopolymer medium with a thickness of about 400 μm as the recording medium.

First, the storage-type SRH experiment was performed. During recording, the hologram was recorded inside a photopolymer medium provided by Kyoeisha Chemical Co [20]. by focusing a beam containing the phase pattern corresponding to the signal data shown in Fig. 8(a). In these experiments, we assumed that the writing phase pattern $\phi^{w}(x, y)$ corresponds to the signal phase pattern $\phi^{s}(x, y)$; i.e., the additional phase pattern $\phi^{ad}(x, y)$ was set to be uniform. The solid and dashed lines enclose the area to be recorded and the area to be used for SNR calculation, respectively, as shown in Fig. 8(b). The intensity distribution of the writing beam is shown in Fig. 8(c). Although the intensity distribution of the writing beam is uniform in the ideal case, that in Fig. 8(c) is inhomogeneous. Because the circular fringes appearing in Fig. 8(c) are caused by the optical elements such as the imager after the beam passes through the recording material, they do not affect the results, whereas the unevenness in the intensity distribution before the recording material causes the inhomogeneous output intensity distribution in the experimental results shown in Figs. 8(d) and 8(e). At the time of readout, the SLM was turned off; i.e., no phase pattern was added to the readout beam. Then, by illuminating the hologram with the readout beam, the intensity pattern was obtained by a CCD camera. The captured intensity distribution is shown in Fig. 8(d). The recorded phase-modulated signal was read out as an intensity-modulated signal with an SNR of 2.1 (3.2 dB), which corresponds to the average intensity ratio between the dark and bright pixels of 1:2.7.

#179394 - $15.00 USD Received 6 Nov 2012; revised 19 Jan 2013; accepted 29 Jan 2013; published 6 Feb 2013

The pixels with stronger and weaker intensities correspond to those with phase levels of π/2 and 0, respectively. This result demonstrates SRH storage operation.

In addition to storage-type SRH, the setup can work as PIC-type SRH by using light beams opposite to those in the storage-type SRH operation described above. In the PIC-type operation experiment, the hologram is written inside the photopolymer by a writing beam with a phase distribution $\phi^r(x, y)$, which is uniform in this experiment. When the hologram is irradiated with the phase distribution $\phi^w(x, y)$ shown in Fig. 8(b), PIC is completed instantaneously, as shown in Fig. 8(e). The SNR of PIC-type operation was 1.9 (2.9 dB), corresponding to an average intensity ratio between the dark and bright pixels of 1:2.3. The result has an inverted intensity distribution compared with that in Fig. 8(d), although the signal phase distribution is the same in both cases. This is because the sign of the phase shift between the writing and readout beams in storage-type and PIC-type operation is reversed, as mentioned above. The result shows that SRH can be applied to high-speed PIC without a speed limit other than that of the transmission velocity of light.

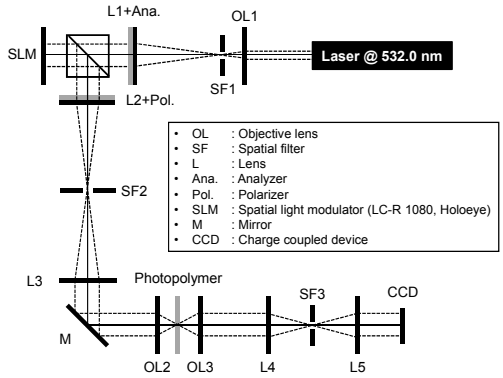

Fig. 7. Experimental setup. Light source was a diode-pumped solid-state laser with a wavelength of 532.0 nm. Focal lengths of L1, L2, L3, L4, and L5 are 150, 200, 200, 100, and 100 mm, respectively.

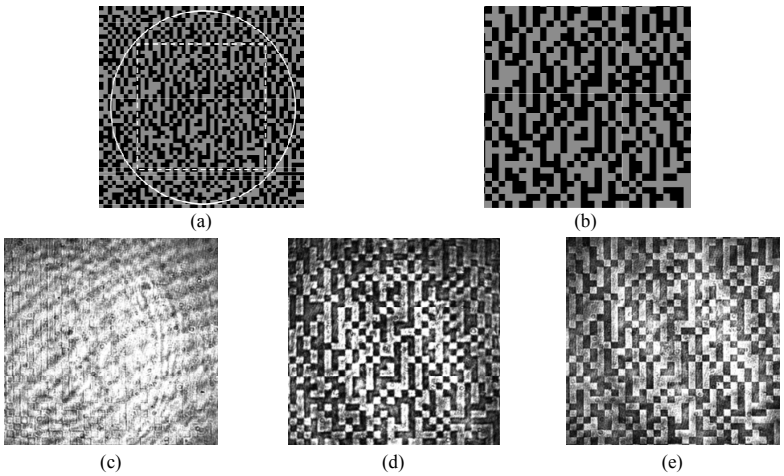

Fig. 8. Experimental results. (a) Signal pattern $\phi^s(x, y)$. Solid and dashed lines enclose the area to be recorded and the area used for SNR calculation, respectively. Dark pixels represent π/2 pixels, whereas brighter pixels represent 0 pixels. (b) Enlarged view of the region for SNR calculation [area enclosed by dashed line in (a)]. (c) Directly captured writing beam, i.e., intensity distribution of $\phi^w(x, y)$. (d) Output intensity pattern in storage-type SRH. (e) Output intensity pattern in PIC-type SRH.

#179394 - $15.00 USD Received 6 Nov 2012; revised 19 Jan 2013; accepted 29 Jan 2013; published 6 Feb 2013

4. Conclusions

A novel hologram recording method, SRH, was proposed. SRH is a purely one-beam holographic recording method in which the signal beam also acts as the reference beam, effectively recording itself in the recording process, and the recorded data are read out by illumination from a properly designed readout beam in the readout process. Because the SRH readout process is based on energy transfer by inter-pixel interference in holographic diffraction, SRH can achieve not only compact optics but also phase-modulated signal reconstruction with no phase detection method. We showed analytically and experimentally that SRH can record and read out phase-modulated binary signals without using a reference beam. In addition, we demonstrated that SRH can be used for holographic data storage and PIC. In SRH-based holographic data storage, compact holographic data storage systems with optics that are interchangeable with those of conventional optical data storage systems can be realized. Furthermore, SRH technology is expected to contribute greatly to the realization of phase-based holographic data storage without using a phase detection method, which is absolutely necessary in conventional schemes. In addition, PIC mode SRH operation provides ultrafast conversion of phase-modulated signals to intensity-modulated signals at the speed of light. In summary, SRH will be applied to a wide field of holography applications owing to its many advantages such as hologram recording without a reference beam and phase-modulated signal processing without the need for phase detection.

Acknowledgment

This work was supported by JSPS KAKENHI Grant Number 24860048.

#179394 - $15.00 USD Received 6 Nov 2012; revised 19 Jan 2013; accepted 29 Jan 2013; published 6 Feb 2013